International Journal of Applied Nanotechnology Research
Volume 4 • Issue 2 • July-December 2019

TiO_2 Nanotubes Transformation Into 4nm Anatase Nanoparticles:

Anodizing Industrial Recycled Titanium for Photocatalytic Water Remediation

Celeste Yunueth Torres López, Centro de Investigación y Desarrollo Tecnológico en Electroquímica, S.C., Mexico

Jose de Jesus Perez Bueno, Centro de Investigación y Desarrollo Tecnológico en Electroquímica, S.C., Mexico

https://orcid.org/0000-0002-7775-405X

Ildefonso Zamudio Torres, Universidad Juárez Autónoma de Tabasco, Mexico

https://orcid.org/0000-0002-1633-2910

Maria Luisa Mendoza López, Instituto Tecnológico de Querétaro, Tecnológico Nacional de México, Mexico

https://orcid.org/0000-0002-3697-1875

Abel Hurtado Macias, Centro de Investigación en Materiales Avanzados A.C., Mexico

José Eleazar Urbina Álvarez, Centro de Investigación y de Estudios Avanzados del Instituto Politécnico Nacional, Unidad Querétaro, Mexico

ABSTRACT

The scope of this work shows novel experimental findings on preparing anatase TiO_2 nanoparticles, first anodizing titanium into an organic media for obtaining TiO_2 nanotubes, and using these as a photocatalytic active electrode in treating water polluted with organic contaminants. The substrates were grit blasted to obtain mechanical fixation of the generated nanotubular TiO_2 structure. This was successfully achieved without diminishment of the nanotubes order and with a self-leveling of the outer surface. A new phenomenon has been investigated consisting of the process of oxidation of the nanotubes in water after anodizing. Along this process, methyl orange added to the aqueous solution was discolored as part of the redox reaction involved. The final state of the modified layer was composed of conglomerates of almost completely crystalline TiO_2 nanoparticles, around 4 nm in size, consisting of anatase. SEM and TEM images show the transition of the amorphous nanotubes (atomic disorder/nanometric order) to crystalline disordered particles (atomic order/nanometric disorder).

KEYWORDS

Anatase, Antibacterial, CO2 Reduction, Dye, Nanomedicine, Nanotechnology, Nanotubes, Photocatalysis, TiO2, UV-Vis, Wastewater, Water Splitting

INTRODUCTION

Today, many materials with different properties have been investigated; this includes nanomaterials, which have the potential to influence modern society in many aspects. These kinds of materials are highly interesting, thus both nanoscience and nanotechnology have become attractive and exciting

DOI: 10.4018/IJANR.2019070102

fields, because nano-systems may not behave like their bulk counterparts. The era of dealing with tiny objects has been gaining momentum in the past few years due to industrial progress, the scientific ability to fabricate, model, and manipulate things with a small number of atoms, and the almost daily discovery of novel size-induced phenomena.

The origin of the size-induced properties in nanomaterials depends on the surface phenomena (extrinsic contribution) and quantum confinement effects (intrinsic contribution). The surface to volume ratio increases rapidly when particle size decreases (Souza Filho & Fagan, 2011). There are many techniques for synthesizing nanoparticles, but study presents the investigation into obtaining them through the synthesis of TiO_2 nanotubes through an electrochemical method (Momeni et al., 2019; Yu et al., 2020). The analysis covers different aspects, such as morphology layer surfaces, shape, and size, chemical composition, crystalline size, catalytic and photocatalytic activity, and morphology before and after catalytic and photocatalytic tests. These analyses detail finding and observing a complete transformation of the structure to 4nm anatase nanoparticles.

There are many studies that have been done on nanomaterials, but those directly related to photocatalysis are primarily associated with TiO_2 or ZnO (Chen & Mao, 2007). TiO_2 is used for many applications, such as sunscreens, antibacterials, chemical sensors, pollutant filters, toner photoconductors, and in optoelectronics (Chen, Wang, Wei, & Zhu 2012; Cui, Gao, Qi, Liu, & Sun 2012; Liang, Luo, Tsang, Zheng, Cheng, & Li, 2012). The main use of TiO_2 is as a white pigment that is put into many products, such as white dispersion paints. Today, it is possible to find several industries throughout the world that are producing different kinds of nano-structured titanium dioxide on a large scale (Khvan, Kim, Hong, & Lee, 2011). The TiO_2 semiconductor material shows a vast number of interesting properties, which are maximized when these belong to the nanostructure. However, one of the emerging and intensively explored properties of this nanostructured oxide is its photocatalytic activity, primarily for the treatment of environmental pollution (Ortega-Diaz et al., 2020).

The photocatalytic phenomena of TiO_2 occur due to the electron-hole formation by absorbing photons with energy equal or higher than the bandgap of this semiconductor plus the potential of the surface. Photocatalysis occurs even the adverse presence of a large number of defects in the crystalline structure, such as oxygen vacancies, interstitial titanium atoms from the donor states, titanium vacancies, and interstitial oxygen atoms from the acceptor states. The electronic condition created in this structural arrangement produces a bandgap, an intrinsic characteristic of semiconductor materials, by the existence of a forbidden gap between the valence and the conduction band. The photocatalytic activity of TiO_2 occurs only when photons with energies greater than its bandgap energy can result in excitation of the valence band electrons, which jump to the conduction band, and then can promote a reaction. The absorption of photons with lower energy or longer wavelengths than the bandgap energy usually causes energy dissipation in the form of heat. The illumination of the photocatalytic surface with sufficient energy leads to the formation of a positive hole in the valence band and an electron in the conduction band (Nakata & Fujishima, 2012).

After the light excitation, the electron hole-created pair could have electronic recombination releasing heat or could be involved in electronic transfer with other species and interact directly, or through some photosensitizers with organic substrates. Either the positive hole oxidizes pollutants directly or water to produce hydroxyl radicals ($^{\bullet}OH$), whereas the electron in the conduction band reduces the oxygen adsorbed on the catalyst (Gelover, Gómez, Reyes, & Leal, 2006). Based on this principle TiO_2 and, more recently, N-TiO_2 (Zhau et al., 2020; Zhou et al., 2020) has received attention in research for the degradation of different organic specimens that are environmental pollutants.

The photocatalysis allows to decompose organic molecules, such as these of azo dyes. The mechanisms and sub-products are many and usually requires higher periods of treatment beyond the decolorization of aqueous solutions for a complete mineralization with H_2O and CO_2 as final products (Zamudio Torres et al., 2016a,b).

BACKGROUND

Pollution from sewage, agricultural, industrial, and domestic water is exhausting water resources, both on the surface, such as lakes and rivers, and underground. Potable water has become insufficient for human consumption and industrial activities. The available water sources are of insufficient quality and at an increasing cost for a growing population. For this reason, technological developments have been sought to identify materials that are useful for treating polluted water, such as titanium dioxide. This material was selected because it has low toxicity, good chemical stability, an accessible cost, and it is chemically and biologically inert.

In general, effluents containing dyes are treated biologically, using adsorption, membranes, coagulation-flocculation, oxidation-ozonation, and Advanced Oxidation Processes (AOP). AOP have been developed to degrade non-biodegradable pollutants from water for human consumption and industrial effluents into non-harmful substances (for example, CO_2 and H_2O). Heterogeneous photocatalysis in combination with TiO_2 and UV light is considered one of the most promising AOPs for the degradation of water-soluble organic compounds (Álvarez et al., 2020; He et al., 2020; Wang et al., 2020). In this way, the degradation of an organic dye by irradiation of light can be generated by three mechanisms: a) by a process of photolysis induced by the energy coming from the radiation source; b) by a photosensitization process where the visible radiation excites electrons of the π bonds of the dye molecule are injected into the conduction band of the semiconductor with the consequent oxidation of the dye; and c) by a conventional photocatalysis process where the promotion of an electron from the valence band to the band conduction of the semiconductor, by action of radiant energy, produces active sites (hollows) for oxidation of the dye (Elhadj et al., 2020; Nguyen, Tran, Tran, & Juang, 2020; Wang & Zhuan, 2020).

There have been many attempts to make TiO_2 more functional by suppressing electron-hole potential recombination at grain boundaries using a variety of methods. These methods included: nanowires (Liu, et al., 2011), nanorods (Huang, Ning, Peng, & Dong, 2012), or nanotubes (Kwon, et al., 2012; Nie, Mo, Zheng, Yuan, & Xiao, 2013; Palmas, et al., 2012), which have been explored as an alternative to nanoparticle-based films. Self-ordered anodic TiO_2 nanotube arrays have especially attracted considerable interest because of their highly aligned geometry and their simple fabrication process (Leiet al., 2013; Liu, Lee, & Schmuki, 2012).

For the production of TiO_2 nanotube layers, different methods have been used, such as sol-gel methods with organic gellants as templates (Arami, Mazloumi, Khalifehzadeh, & Sadrnezhaad, 2007), pre-deposited hydrothermal TiO_2 (L. Cui et al., 2012), microwave-assisted hydrothermal (Cui et al., 2012), sonochemical (Arami et al., 2007), microemulsion (Y. Li, L., Li, C., Li, Chen, & Zeng et al., 2012), solvothermal (Wang, Yang, Wang, Huang, & Hou, 2012), atomic layer deposition (ALD) (Meng et al., 2013), seeded growth method (Tian, Voigt, Liu, McKenzie, & Xu, 2003), by means of ionic liquids (H. Li et al., 2011), and anodized Ti (Gong et al., 2001), among others. The anodized Ti for obtaining TiO_2 nanotubes offers better control over their dimensions and homogeneity. This is carried out in fluoride-based electrolytes (Gong et al., 2001; Lai, Gong, & Lin, 2012).

In 2001, D. Gong et al. (2001) first developed titania nanotube arrays self-organized into a Ti substrate by potentiostatic anodic oxidation using HF solutions as an electrolyte and pure Ti plate as the substrate. As a consequence, this led to the rise of the research on TiO_2 nanotube arrays. The researchers' special nanoarchitecture offered a high inner surface without a corresponding decrease in geometric and structural order (Shankar, Varghese, Mor, Paulose, Varghese, & Grimes, 2008). These oriented structures make them excellent electron percolation pathways for a charge transfer vector between interfaces and offer improved properties for applications in many fields, such as solar cells, photocatalysis, photolysis of water, and hydrogen sensors (Johns, Roberts, & Owen, 2011).

The primary use of TiO_2 is photocatalysis. One disadvantage of TiO_2 nanoparticles is that they can only use a small percentage of sunlight for photocatalysis. Practically, there exists an optimal size

for a specific photocatalytic reaction. This work is based on the results obtained after the degradation of methyl orange using TiO_2 nanotubes.

New materials and technologies have been sought for application in treatment systems to remove organic pollutants from water. The use of photocatalysis in TiO_2 (titania) is proposed as an alternative with great potential and has been widely researched for the decomposition of these pollutants.

When obtained by chemical synthesis and commercially in powder form, TiO_2 is desired to give it a nanotube type structure grown directly from the titanium metal for use in continuous processes having water fluxes and the ability to recover photocatalytic surfaces easily. In addition, unlike conventionally obtained structures, with heat treatment at about 450°C, for over half an hour, it is sought to generate nanotubular structures at room temperature. Some of the advantages of nanotubes compared to nanoparticles include the following:

- The effective active area in contact with the solution. Due to the cylindrical nature of the nanotubes, there is a greater contact of the solution with said structures, managing to penetrate the NM into the nanotubes, generating an increase in the possibilities of degradation of the dye;
- The high order;
- The support on titanium, which offers greater advantage to be used with water in continuous processes.

The three points above are considered advantages over nanoparticulated TiO_2 as the characteristics of the nanotubes provide a superior catalytic decomposition of organic components because they allow the easy diffusion of contaminants within the TiO_2 nanotubes. In addition, the use of nanoparticulated TiO_2 implies that once the photocatalysis process is finished, it is necessary to clean the water subjected to the treatment, since the nanoparticles will be suspended and will require additional stages, or it is not possible. On the other hand, if TiO_2 nanotubes are used, it is no longer necessary to apply an additional cleaning process to the water treated by the photocatalytic process. Additionally, TiO_2 nanotubes grow directly from metallic titanium pieces in any shape and can be re-processed to create new photocatalytic surfaces just by polishing and anodizing. So, the photoactive surfaces can be recycled.

This study seeks to propose alternative solutions to solving the contamination of some organic compounds in water through the use of metastable nanotubular structures of TiO_2. Specifically, the manufacture of titanium plates with nanotubular TiO_2 surfaces. The discoloration and degradation of aqueous solutions of methyl orange (NM) was evaluated in two ways: photocatalytic and catalytic. For the photocatalytic pathway, an experimental setup was performed for exposure to UV light and subsequent discoloration and degradation of NM. While for the catalytic pathway, only a dark environment was necessary to generate the aforementioned effects.

The model compound to be degraded was NM, a simple structure dye with a single azo bond (N = N), frequently used as an indicator of the photocatalytic activity of titania (Boczar, Łęcki, & Skompska, 2020: Florez et al., 2020; Zhiyong, Ruiying, Runbo, Zhiyin, & Huanrong, 2020). NM is an organic substance used as a dye in the textile industry and as an acid-base indicator. It has been shown that this substance is not biodegradable when present in water, which is why photocatalysis is proposed for use; photocatalysis, which belongs to the AOP, has the function of degrading compounds that are hard to be degraded organically (aerobically or anaerobically).

Finally, in general terms, photocatalysis in TiO_2 is considered to be an alternative with great potential and has been widely researched for the decomposition of organic pollutant molecules in water. However, the study of nanotubular structures of TiO_2 by using anodizing and dissolution on titanium is a relatively new area of research in photocatalysis.

EXPERIMENTAL

TiO_2 nanotubes were synthesized through anodizing-dissolution. The preparation of the Ti plates for the anodizing process began with the removal of any rust present by polishing. Then, the Ti plates were subjected to a sandblasting process provided by the Sandblast Horus Group Ltd., Tezca Mark, for generating a rough surface, which was proposed to anchor the nanotubes adequately.

The system for anodizing was an organic medium, which consisted of the following: Electrolyte (ethylene glycol 98% v/v, H_2O 2% v/v, NH_4F 0.3% wt/%) and Ti plates (97.5% Ti, 2.42% C, 0.08% Sn). The anodizing time was variable and the times were 2, 4, 8, and 16 h. Among the times, 2 h and 4 h resulted in a better degradation effect (Figure 7). A voltage ramp of approximately 100 mV/s (6 V/min) was used, starting from 6 V, and increasing it to 60 V (main potential used in the TiO_2 nanotubes generation process).

The experimental setup consisted of: a) an open transparent polypropylene container with a capacity of 4L; b) a central Ti plate as a cathode (13 x 9 cm, thickness of 1 mm), the immersed area was typically 4 x 9 cm, and; c) two Ti plates as anodes (4 cm x 3 cm, thickness of 1 mm), one per each side of the cathode, with a 2 cm separation between anode-cathode-anode and an immersed area typically of 2.5 cm x 3 cm (7.5 cm^2).

After obtained, TiO_2 nanotube layers were used to treat methyl orange aqueous solutions catalytically (without UV light) and photocatalytically (with UV light). The methyl orange ($C_{14}H_{14}N_3NaO_3S$, Acros Organics brand), with a concentration of 20 mg/L, was used as a model contaminant. These tests were performed with 15 mL of the solution put into polypropylene bottles, where anodized Ti plates were immersed, and later stored into the darkness within a container.

For photocatalytic degradation tests, methyl orange aqueous solutions were placed in open plastic containers. The anodized Ti plates were placed into the solution, the container was placed into a special cell for photocatalysis (closed, black PVC container) and subjected to artificial UV light with a mercury UV lamp (GE germicide lamp, model G15T8, 15 W).

TiO_2 nanotubes were generated in an organic medium (0.3 wt/% NH_4F and 2 v/% H_2O in ethylene glycol, 60 V) with various anodizing times (30 min, 2 h, 4 h, 8 h, and 16 h).

There is a relationship between the pore diameter, the wall thickness, and the anodizing voltage, which, among other factors, form part of the process of forming the TiO_2 nanotube arrays on the surface of the titanium (Roy, Berger, & Schmuki, 2011). The mechanism is:

1. The formation of a compact layer of titanium dioxide occurs in the first step. It is formed due to the interaction of metallic Ti with O^{2-} and OH^-, present into the solution, under an externally applied electric field (reactions 2 and 3):

$$Ti^{4+} + 2H_2O \rightarrow TiO_2 + 4H^+$$

2. With the TiO_2 layer formed on the anode in the vicinity of this, the TiO_2 surface reacts with fluoride ions, with the help of the electric field, forming the complex $[TiF_6]^{2-}$ dissolved in water, resulting in surface cracks:

$$TiO_2 + 6F^- + 4H^+ \rightarrow TiF_6^{2-} + 2H_2O$$

3. Fractures become larger pores, and the pore density increases. Subsequently, the pores become evenly spread over the surface (Y. Liu et al., 2011);
4. When the rate of oxide growth on the metal-oxide interface and the dissolution rate of oxide in the oxide-electrolyte interface are equal, the thickness of the barrier layer remains unchanged;

5. The length of the nanotubes increases as long as the ratio of electrochemical oxidation remains equal to the ratio of chemical dissolution in the upper surface of the nanotubes. Thus, it produces a porous, self-organized structure.

Various causes influence the photocatalytic efficiency in nanotubular titania surfaces, among others, the manufacturing process, in which the factors are: current intensity, the electrolyte used, impurities, treatment temperature, dissolved oxygen, experimental setup, etc.

To evaluate the photocatalytic activity of titanium dioxide, a single dye having a molecule with a single link azo (N = N) was used, named methyl orange (MO).

Some of the unusual conditions employed to produce the nanotubular structures:

1. **Sandblasting:** Before applying this technique, titanium plates were cleaned with a wire brush to remove corrosion on the surface. After cleaning, the application proceeds to sandblast (only to the anodes). The pressure used to accomplish the surface attrition was 100 kg/cm^2, for one min per side of each Ti plate. The abrasive material used was Al_2O_3 with an average particle size of about 2.5 mm. The principal reason for using sandblasting was to increase the adhesion of the modified nanotubes layers, and to resist adverse mechanical conditions. An example could be the continuous flow of water. This treatment was necessary because, after the first tests of titanium anodizing (without sandblasting), the results revealed that the layers made of the nanotubular structures had poor adhesion, had fractures, and detached easily;
2. **Water dosing for the system:** The experimental setup consisted of an open vessel, which allowed evaporation, along with water consumption, by electrolysis required for providing oxygen and acidity to the bottom of the nanotubes. This made it necessary to continually add water into the system. This was done by dripping water in at a rate that could compensate for the loss of water, and that maintained the same solution level. In addition, this change in the process, as a favorable consequence, avoided a rise in the electrical resistivity of the system. The conductivity of the solution was monitored and controlled, which resulted in indications of a balance among TiF_6 resulting from the reaction, the addition of NH_4F for maintaining the fluoride level, and constant water addition. After completing each anodizing process, solutions were stored. Usually, during a period that allowed enough time for precipitation of a crystalline compound to occur. These crystals were composed of fluorine, ammonium, and titanium (Figure 8). After separating the precipitate, the ethylene glycol solutions were re-used for anodizing. During all of the experiments, the implementation of magnetic stirring into the system was done. This allowed a mass transport, improving the homogeneity of the species concentrations in the solution;
3. **Voltage ramp:** Applying an initial voltage ramp has been shown to promote the development of a network of interconnected cavities from the early stages of the process. This helps to release stress at the interface metal/metal-oxide (M/OM) and aids in the retention of the titania layer on top of the titanium substrate. Since, at the beginning of the experiment, the electrode located close to the solution was without an oxide layer, it, therefore, required less current density;
4. **Adding NH_4F to the electrolyte:** When the solution was created from new or pure ethylene glycol, usually a 0.3% w/w of NH_4F was added, according to calculations based on the conditions of the electrolyte. However, when the electrolyte was re-used, it was necessary to add NH_4F. Subsequent additions to use baths were done to maintain the chemical dissolution of TiO_2. Some tests were realized for comparing nanotube layers obtained after many were anodized in the same ethylene glycol bath. It was found that the bath could be used four times without detriment in the conditions or characteristics of the resulting nanotube layers. This was performed with consideration for the material additions and monitoring the process parameters;
5. **Ultrasonic cleaning (sonication) of the nanotube-modified Ti plate surface:** After anodizing Ti, it was necessary to apply sonication, which involves the propagation of high-intensity sound

waves in liquid media. This is one of the most efficient methods of cleaning and results are non-abrasive and do not leave residues of chemical solutions on the substrates.

The application of ultrasonic cleaning was intended to eliminate any remaining adsorbed species after the anodizing process on the modified titanium plate. This cleaning was conducted by immersing the nanotube-Ti plate in a beaker containing deionized water.

RESULTS AND DISCUSSION

SEM and HRTEM Analysis of Nanotubes

Tubular structures were observed using a scanning electron microscope (SEM), which shows TiO_2 nanotubes formed, generated during an anodizing-dissolution process in organic media. Figures 1A through 1D provide SEM images that show TiO_2 layers and nanotubes structures.

Figure 1A shows an area of 1.0 μm^2, where it is possible to see 32 nanotubes, wherein 29 of these are surrounded by 6 nanotubes and 3 are surrounded by 5 nanotubes. Therefore, based on such observation, the hexagonal packing factor was 0.92. Thus, 92% of the nanotubes had six first neighbors. In this area, the nanotubes were not perpendicular to the surface plane but deviated to the left. This was something typical for the nano-structures with substrates subject to sandblasting.

Figure 1. Four SEM images corresponding to A) sandblasted and anodized Ti substrate, Figures 1B through 1D corresponding to anodized Ti without sandblasting pretreatment.

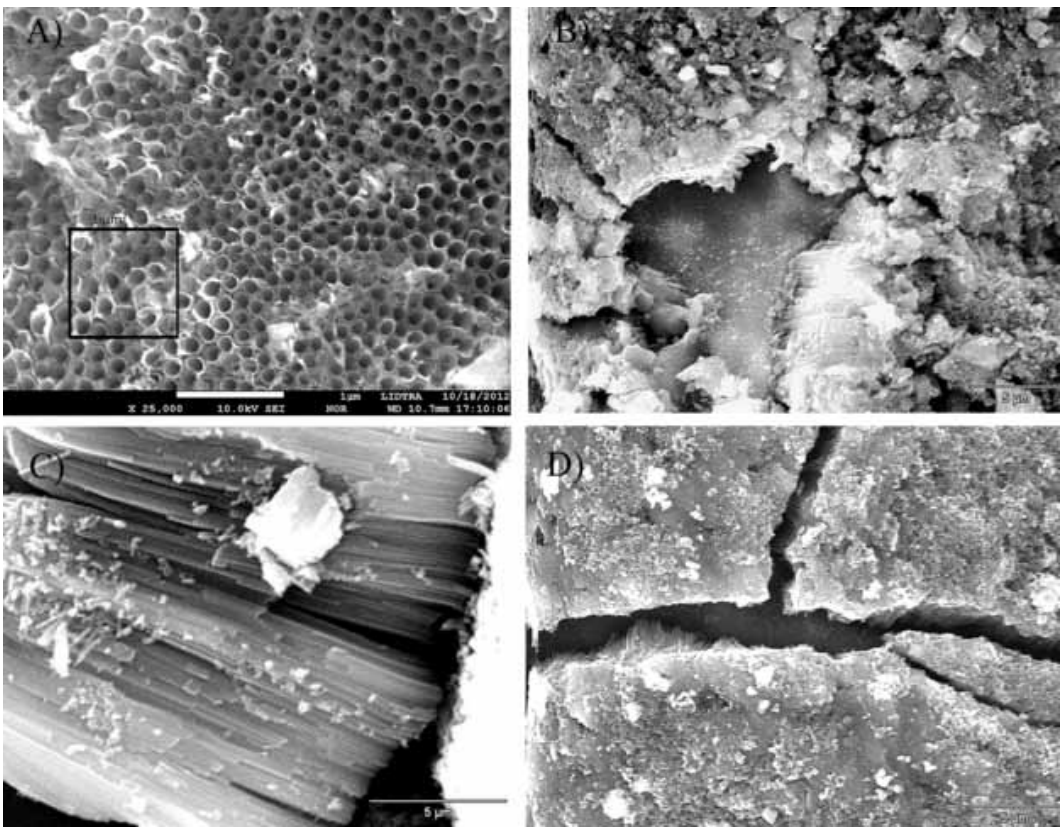

For those nanotubes normal to the surface plane, the calculated wall thickness and pore size were approximately 10-20 nm and 110-140 nm, respectively.

Figures 1B and 1D show fractures on a top modified layer, which shows nanotubes formed at the bottom, constituting a second modified layer. This was changed by using sandblasting as shown in Figure 1A. The thickness depends on different parameters, such as time, but typically was approximately 10 μm per 2 h of anodizing. Figure 1C shows a detached fragment of the nanotube layer with a thickness of approximately 17.6 μm.

TEM was used for samples previously used in water treatment. The nanotubular structures obtained by means of anodized titanium, after the treatment, resulted in different morphology in comparison to other works reported. They were metastable due to their composition: fluorine, ammonium, and titanium. Figure 2 shows four TEM images that present the nanotubes transformation to nanoparticles. Figure 2-B, 2-C, 2-D present fuzzy nanotubes.

Figure 2A (0.2μm) is shown in the top-left photo, Figure 2B (0.5 μm) is shown in the top-right photo, Figure 2C (200 nm) is shown in the bottom-left photo, and Figure 2D (50 nm) is shown in the bottom-right photo.

The authors propose that those structures underwent a transformation from a structure made of fluorine/ammonium/titanium, by slowly oxidizing in water, until reaching a titanium oxide.

Figure 3 shows that the material is highly crystalline. The crystallite size was determined by Scherer's equation (eq. 1) and the size was approximately 4 nm:

$$\tau = \frac{K\lambda}{\beta \operatorname{Cos}\theta}$$

Figure 3A (10 nm) is shown in the left photo; Figure 3B (2 nm) is shown in the right photo.

This was first observed on samples that had higher percentages of discoloration of methyl orange aqueous solutions, corresponding to 2 h of anodizing time (Figures 2A and 2B). The samples were immersed in water containing methyl orange for approximately around four days. This caused a solution discoloration, but also a surface change. The nanotubes layer was modified to a thick, white, powdery layer.

A High-resolution transmission electron microscopy (HRTEM) analysis was performed on the sample after 2 h (Figures 2A and 2B) and 4 h (Figures 2C and 2D) of anodizing without the application of a heat treatment. This implies the generation of the anatase nanoparticles from contact with the aqueous solution. These micrographs show the presence of nanotubular structures with apertures of nanotubes of approximately 120 nm with lengths of approximately 0.5 μm. The nanotubes apertures measured by HRTEM (120 nm) coincided with that obtained from SEM (110 -140 nm).

In those cases where the nanotubular structure was desirable, heat treatments of approximately 450°C were applied for 30 min. The crystallite size was approximately 25-40 nm.

Chemical Composition and Crystalline Sizes Determination

In addition to identifying the desired phase (anatase) for photocatalytic processes by means of X-ray powder diffraction (XRD), it is possible to determine the chemical composition in weight percent (% wt) and the size of the crystals formed (nm) by using the Rietveld method. This is considering only the crystalline part of the samples and excluding those elements below 10,000 ppm. Figure 4 shows two diffractograms, one corresponding to a Ti-treated plate with methyl orange aqueous solution, and another corresponding to a similar sample, but heat-treated. In addition, it shows the anatase reference pattern JCPS 21-1272.

This confirmed that it was possible to obtain the anatase phase without heat treatment only by oxidation in contact with the aqueous solution of NM (nitromethane). In both cases, tests with and without the application of UV light (for 4 h) were performed. Finally, there was a substantial crystallite

Figure 2. Four TEM images corresponding to nanotubes after water exposure for four days. The fuzzy structure indicates the transformation of nanotubes to a particulate system.

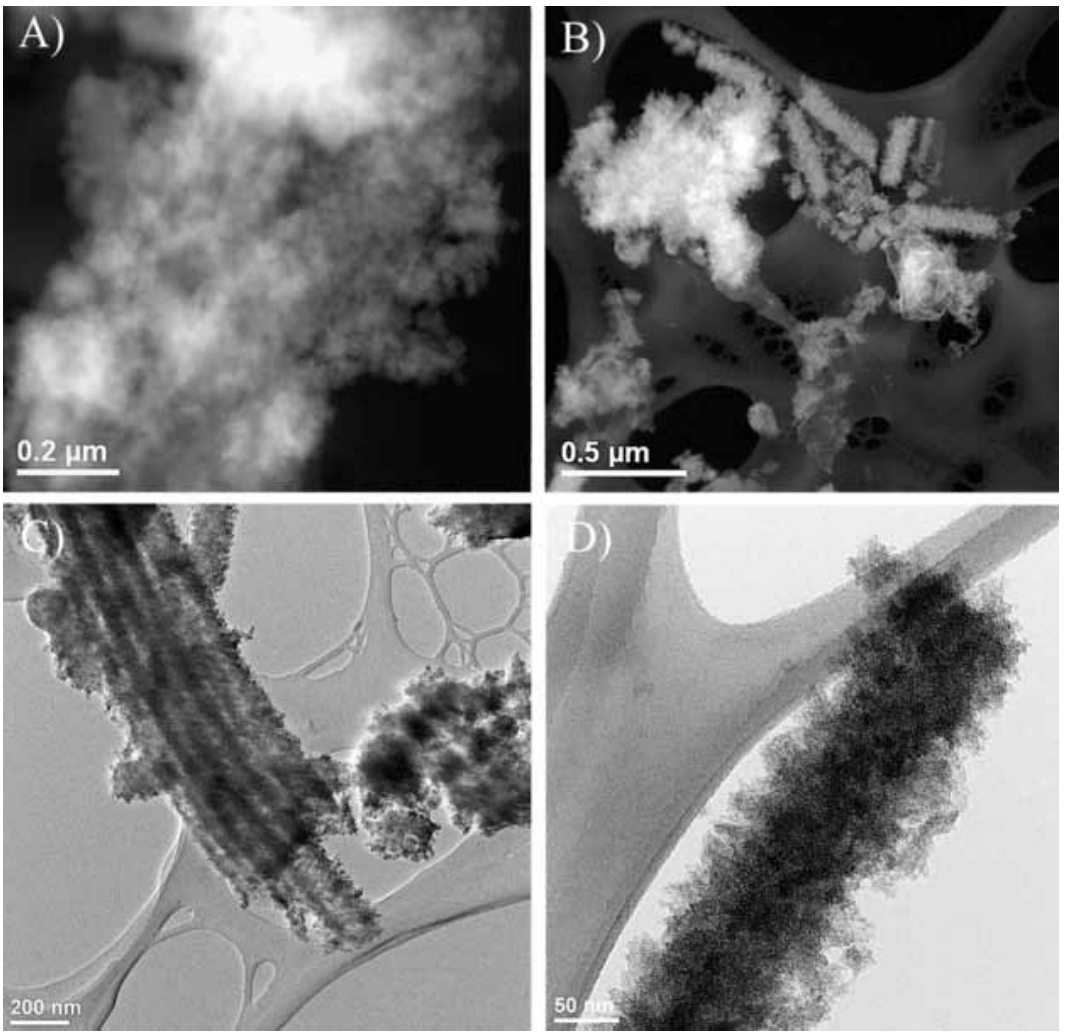

size difference observed in the anatase phase, with and without heat treatment. The larger crystallite size (26.8 nm) was obtained by using temperature in order to modify samples and a smaller size (4 nm) was obtained by immersion in aqueous methyl orange solutions.

Discoloration of Methyl Orange (MO)

For determining the concentration of MO, the UV-vis (ultraviolet–visible absorption) spectra (absorbance vs. concentration) was used to acquire data on aqueous dye solutions with the following concentrations: 5, 10, 20, 25 and 30 mg / L. The main absorption band was located at 463 nm (see Figure 5, label MO). The absorbance for all of the concentrations was taken at the wavelength used for the calibration curve. Those samples were not exposed to UV.

Figure 5 show the absorbance spectra for a series of samples used in the catalytic tests. Sample M1 was obtained by anodizing the titanium for 4 h, but it was used previously in a discoloration test. Sample M2 was obtained by anodizing the titanium for 4 h, but it was not dried in air before

Figure 3. HRTEM images corresponding to nanotubes after water exposure for four days. The fuzzy atoms distribution indicates the transformation of the amorphous nanotubes (atomic disorder/nanometric order) to crystalline disordered particles (atomic order/nanometric disorder).

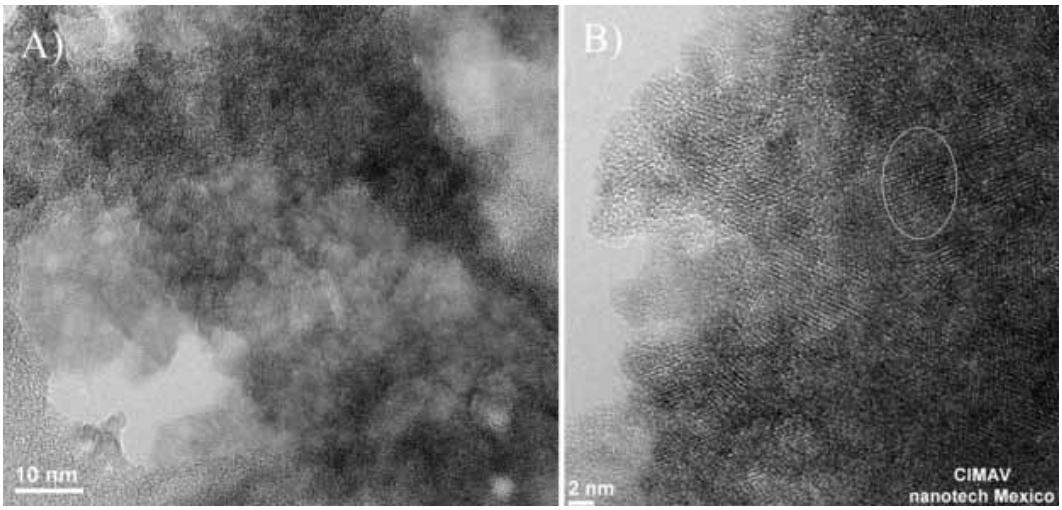

Figure 4. Diffractograms of anodized titanium plates with heat and water treatments. Black squares indicate the anatase peaks. The other peaks correspond to metallic titanium.

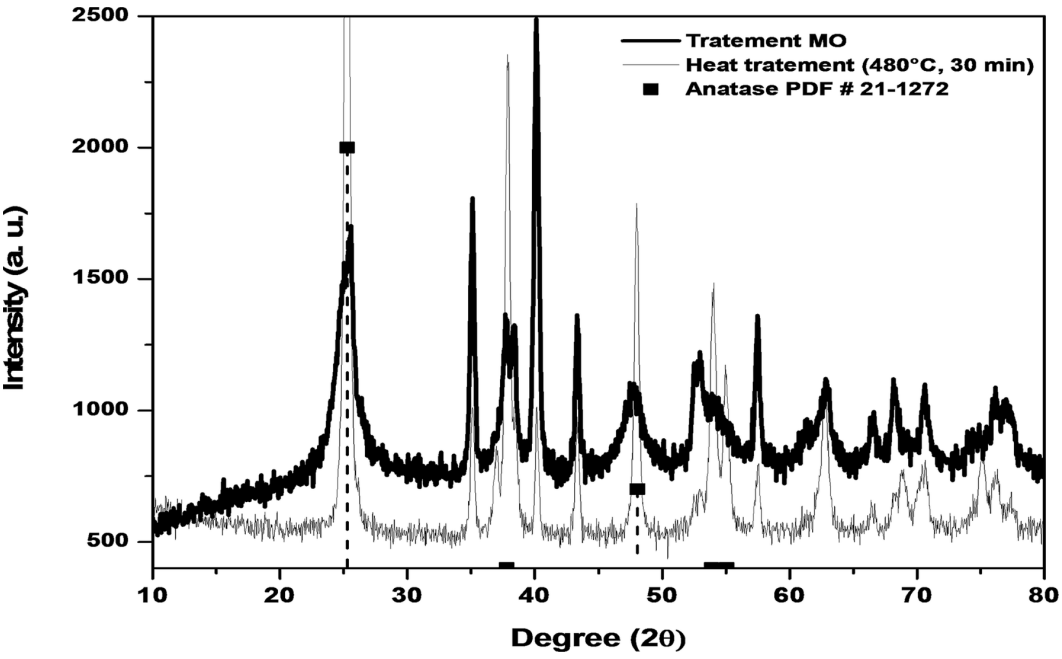

discoloration tests, but instead, kept in ethylene glycol. Samples M3 through M7 were obtained by anodizing the titanium for 2, 4, 8, and 16 h, respectively.

The samples were not exposed to UV, thus the discoloration was attributed to a collateral effect of the oxidation process for the nanotubes. Samples M2 and M3 showed a higher degree of discoloration,

Figure 5. UV-vis analysis shows spectra corresponding to the process of methyl orange discoloration during the process of nanotubes oxidation and their transformation to anatase nanoparticles.

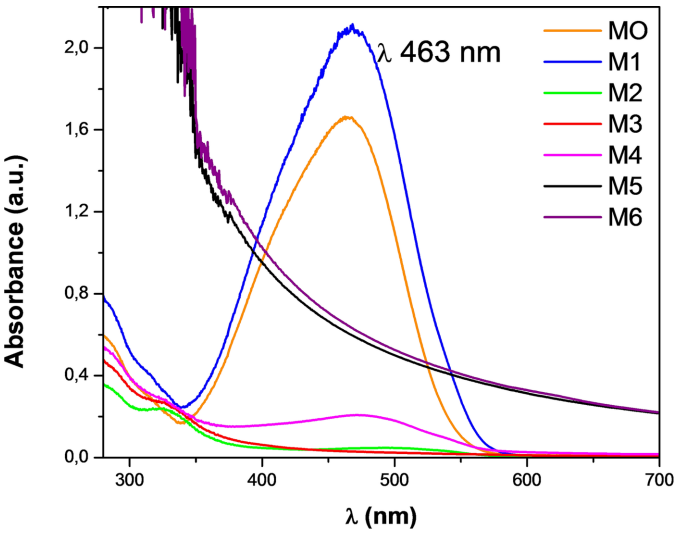

corresponding to 4 h and 2 h of anodizing, respectively. The contact time with the solution for all samples was approximately four days. Samples M2 and M3 accomplished the discoloration in two days. The authors propose that the oxidation process in those two samples was due to the nanotubes' layer conditions, such as the fluorine/ammonium/titanium bonds and ratios.

With regard to the samples that underwent 8 h and 16 h of anodizing, it was noted that the discoloration of the methyl orange solutions were not as effective as the results for samples M2 and M3. It is important to note that the M1 sample increased nitromethane coloring. The orange color change began increasing its intensity with a deep red tone; it was previously used in another discoloration test, which was the primary difference. The other samples only diminished solutions color. Nonetheless, this capacity for discoloring the methyl orange solution only occurred during the oxidation of the nanotubes layer process. After it was complete, the samples lost this effect without UV exposure. Therefore, it was possible to observe a loss of bleaching effect on MO when a sample was used more than once. Since the transformation creates anatase particles, they become photocatalytic, but with poor cohesion among particles or adhesion to the substrate. The samples M5 and M6, despite not having the dye absorption band, had a high baseline due to turbidity caused by the detaching of TiO_2 nanoparticles that remained as a permanent colloid in the aqueous solution.

Kinetic Analysis

The process degradation was adjusted to a kinetic model and a constant rate of reaction kinetics was obtained using the Langmuir-Hinshelwood equation (1). This equation applies to low dye concentrations. The concentration of MO (20 mg/L) was appropriate for the use of this equation:

$$\ln\left[\frac{C_0}{C}\right] = k_{app}t$$

Equation (1) was used by testing the reaction. It was plotted as ln [C_0/C] vs. time (t) and 1/C vs. time (t), which represents reactions of first and second order, respectively.

Figure 6 shows a correlation coefficient very close to 1 ($R^2 = 0.9933$). Therefore, it provides a very good fitting of the reaction to an equation of the first order. In other words, the order of reaction was 1. The experimental data were indicated as square dots. The black straight line is for eye-guide and the blue curve fits the real data. The figure shows only five experimental data and the curve was drawn for fitting these dots. It is an isotherm because the temperature was kept unchanged. There was evolution of the system as the dye was decolored. So, the kinetics refers to this variation of dye color intensity.

Figure 6. Fitting of the ln [C_0/C] vs. Time (t) plot corresponding to the discoloration of methyl orange in water using nanotubes plates

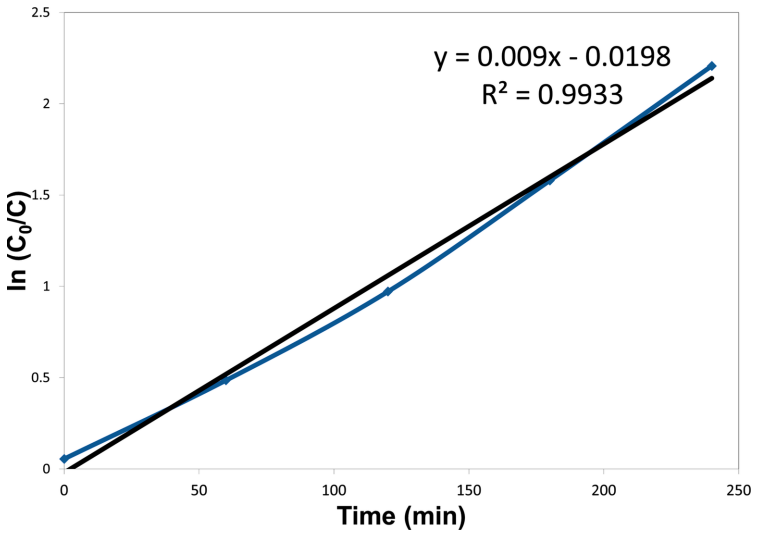

Catalytic and Photocatalytic Tests

Photocatalytic Tests

Photocatalytic tests performed were of two kinds:

1. Test with 1 h of exposure to UV light and 4 days of nanotube-modified plates in contact with the MO solution;
2. Test with 4 h of exposure to UV light. This was the time required for discoloration of the MO solution with the experimental setup used.

In these tests, modified surfaces were exposed to ultraviolet light within MO solutions. This was performed in a closed cell for photocatalysis. The time of exposure to UV light was 1 h, whereas the contact time with the solution of MO was 96 h (four days, as in the tests without UV exposure). MO discoloration was quantified by UV-vis analysis.

Discoloration Effect

UV-vis analysis showed the effect of MO via photocatalytic discoloration. The degree of discoloration observed in samples over time generated six different conditions. Figure 7 shows the absorbance spectra for the series of photocatalytic tests performed. Samples M3 and M4 were those that had

a higher degree of decolorizing, corresponding to 2 h and 4 h of Ti anodizing, respectively. In the cases of tests on samples that underwent 8 h and 16 h of Ti anodizing (M5 and M6, respectively), discolorations were not as effective as results noted in samples M3 and M4.

It is important to note that sample M1 increased MO coloring. Again, this modified titanium plate sample was previously used in another discoloration test. It was possible to observe a loss of bleaching effect on the MO. As mentioned, the discoloration effect on the dye can be observed only when the surface was not previously used. Once the oxidation of the layer was complete, such effect ends.

Figure 7. UV-vis spectra of solutions with discoloration of methyl orange in a photocatalytic process

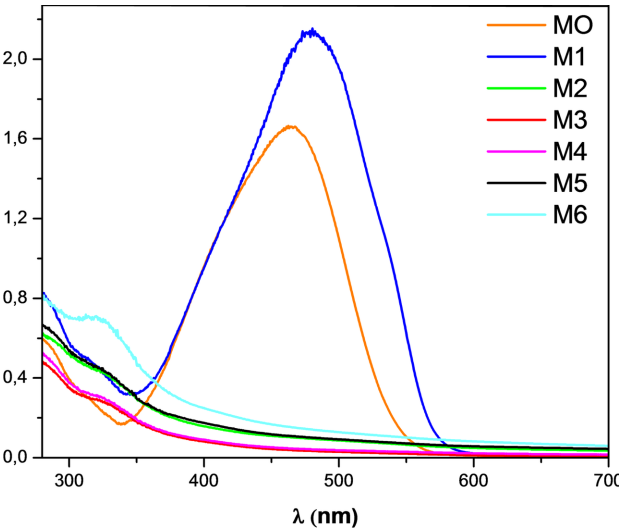

Titanium plates can be easily cleaned by removing the TiO_2 nanoparticles formed during the oxidation/discoloration effect, which is possible using sonication for approximately 20 min. This action frees the titanium plates and makes them available for use again to repeat the anodizing process.

Comparison Between Catalytic and Photocatalytic Tests

In previous sections, the catalytic and photocatalytic effects by contacting nanotubes modified titanium plates with the aqueous solutions of MO were analyzed. In this way, two kinds of tests were conducted, one catalytic and the other photocatalytic. Based on the results, both processes resulted in discoloration of the MO solution. The photocatalytic discoloration was obtained within 1 h of exposure to UV light. However, the time required to perform a test with the catalytical process was 96 h. This limits its use, together with the fact of a single-use for each sample. On the other hand, such an effect is a new observation. The collateral discoloration effect was a way to quantify and follow the transformation of the nanotubes layer by oxidation, and their loss of ammonium and fluoride that formed part of the structure.

Analysis of Precipitate Formed After Anodizing in Organic Media

During the generation of nanotubes by oxidation-dissolution of Ti-TiO_2 an organic bath was used. Their composition was: ethylene glycol 98% v/v, H_2O 2% v/v, NH4F 0.3 wt/%. These electrolytes were re-used several times, according to the procedure described in the experimental section. After being used approximately four times, the solutions were saturated. The solutions were stored, which

allowed for an accumulation of a precipitate. The white powdery precipitate was abundant. It also was easy to remove, allowing re-use of those solutions for anodizing.

Figure 8 shows the fitting by the Rietveld method using the TOPAS 4.2 software. The lines at the top correspond to the experimental diffractograms and the fitting. The gray line corresponds to the difference between those two.

Figure 8. The fitting of a diffractogram corresponding to a white precipitate formed at the solutions used for anodizing titanium plates. This crystalline compound was identified as $(NH_4)_2TiF_4O$.

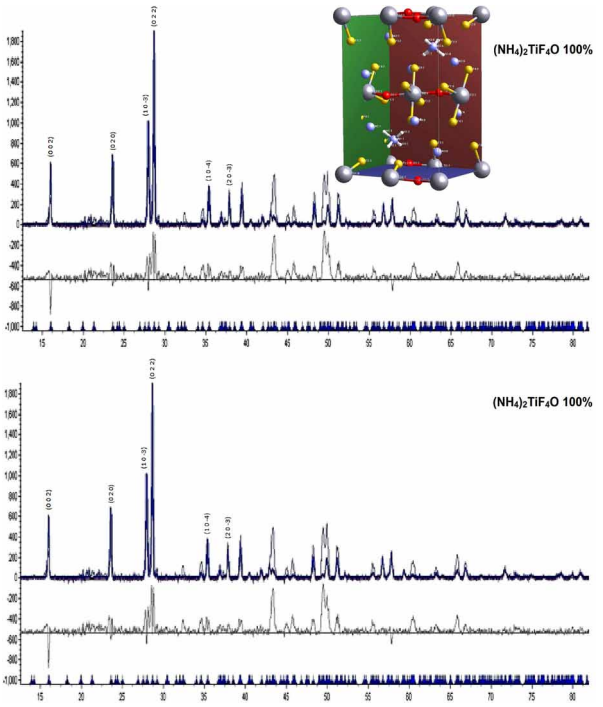

The white precipitate was formed into the solutions used for anodizing titanium plates. The time, obtaining this precipitate depended upon the concentration and storage conditions of the bath previously used. After separation and cleaning, the precipitate was analyzed by X-ray Diffraction (XRD). This allowed a determination of composition. According to the XRD, the compound identified in the precipitate formed after anodizing titanium plates was $(NH_4)_2TiF_4O$, ammonium fluoride titanium oxide, which corresponded to 100% of its composition. Its unit cell is displayed as an insert in Figure 8.

An amorphous variant of the compound $(NH_4)_2TiF_4O$ is proposed as forming the nanotube structure shown in the SEM images, which transforms into anatase nanoparticles, as shown in the HRTEM images, by oxidation of such compound.

CONCLUSION

Nanotubes structures were generated by anodizing titanium plates using an organic solution (NH_4F 0.3 wt/%, H_2O 2% v/v, $C_2H_6O_2$ 98% v/v) employing a voltage ramp of 6 V/min and, finally, maintaining 60 V, which was the working potential of the anodizing process. The dimensions of the nanotubes

generated at room temperature were nanotube openings of 110–140 nm, wall thickness 10–20 nm, length 5–20 μm.

The nanotubular structures generated were metastable. Their procurement was under some changes incorporated into the process, such as: sandblasting of the titanium plates, continuously adding water to the system, constant agitation of the electrolyte, the addition of ammonium fluoride to compensate its consumption, re-use of solutions, and voltage ramps. Additionally, long periods of immersion for the modified layer plates into the aqueous MO solution (20 mg/L), ranged from 4 to 96 h. Samples were then analyzed by XRD, SEM, and HRTEM, where anatase nanoparticles were identified, substituting the nanotube structures.

XRD showed that before contacting the MO aqueous solution of modified titanium plates, no anatase structure appeared. However, after a slow oxidation process within an aqueous MO solution, it was possible to observe anatase TiO_2. This was independent of UV exposure. Furthermore, by employing XRD, a marked difference was observed in crystallite sizes with and without heat treatment, resulting in sizes of 26.8 and 4.7 nm, respectively. According to the discoloration rates obtained, the test using 4 h of exposure to UV light resulted in 95.5% of discoloration. TEM showed a conversion of nanotubes to TiO_2 nanoparticles without heat treatment. An amorphous variant of the compound $(NH_4)_2TiF_4O$ is proposed as forming the nanotube structure that is shown in the SEM images, which transforms into anatase nanoparticles, as shown in the HRTEM images, by oxidation of such compound.

ACKNOWLEDGMENT

This research was supported by the National Council of Science and Technology CONACYT [grant CEMIE-Sol No. 207450 P18 and P62; gran National Laboratory of Graphenic Materials LNMG No. 299124]; the World Bank Group and Energy Secretariat (SENER) [grant number 002/2017-PRODETES-PLATA].

REFERENCES

Álvarez, M. A., Ruidíaz-Martínez, M., Cruz-Quesada, G., López-Ramón, M. V., Rivera-Utrilla, J., Sánchez-Polo, M., & Mota, A. J. (2020). Removal of parabens from water by UV-driven advanced oxidation processes. *Chemical Engineering Journal*, *379*, 122334. doi:10.1016/j.cej.2019.122334

Arami, H., Mazloumi, M., Khalifehzadeh, R., & Sadrnezhaad, S. K. (2007). Sonochemical preparation of TiO_2 nanoparticles. *Materials Letters*, *61*(23-24), 4559–4561. doi:10.1016/j.matlet.2007.02.051

Boczar, D., Łęcki, T., & Skompska, M. (2020). Visible-light driven Fe_xO_y/TiO_2/Au photocatalyst – synthesis, characterization and application for methyl orange photodegradation. *Journal of Electroanalytical Chemistry (Lausanne, Switzerland)*, *859*, 113829. doi:10.1016/j.jelechem.2020.113829

Chen, J., Wang, H., Wei, X., & Zhu, L. (2012). Characterization, properties and catalytic application of TiO_2 nanotubes prepared by ultrasonic-assisted sol-hydrothermal method. *Materials Research Bulletin*, *47*(11), 3747–3752. doi:10.1016/j.materresbull.2012.06.029

Chen, X., & Mao, S. S. (2007). Titanium dioxide nanomaterials: Synthesis, properties, modifications, and applications. *Chemical Reviews*, *107*(7), 2891–2959. doi:10.1021/cr0500535 PMID:17590053

Cui, C. X., Gao, X., Qi, Y. M., Liu, S. J., & Sun, J. B. (2012). Microstructure and antibacterial property of in situ TiO2 nanotube layers/titanium biocomposites. *Journal of the Mechanical Behavior of Biomedical Materials*, *8*, 178–183. doi:10.1016/j.jmbbm.2012.01.004 PMID:22402164

Cui, L., Hui, K. N., Hui, K. S., Lee, S. K., Zhou, W., Wan, Z. P., & Thuc, C.-N. H. (2012). Facile microwave-assisted hydrothermal synthesis of TiO_2 nanotubes. *Materials Letters*, *75*, 175–178. doi:10.1016/j.matlet.2012.02.004

Elhadj, M., Samira, A., Mohamed, T., Djawad, F., Asma, A., & Djamel, N. (2020). Removal of Basic Red 46 dye from aqueous solution by adsorption and photocatalysis: Equilibrium, isotherms, kinetics, and thermodynamic studies. *Separation Science and Technology (Philadelphia)*, *55*(5), 867–885. doi:10.1080/01496395.2019.1577896

Florez, D. M. M. G., Ale, R. B. G., Idme, A. F. H., Alarcon, L. A. L., Huallpa, E. A., Castro, Y., Apestegui, P. G. R., & Rodriguez Rodriguez, J. M. (2020). SiO_2-TiO_2 Films Supported on Ignimbrite by Spray Coating for the Photocatalytic Degradation of NO_x Gas and Methyl Orange Dye. *International Journal of Photoenergy*, *2020*, 1–6. Advance online publication. doi:10.1155/2020/4756952

Gelover, S., Gómez, L. A., Reyes, K., & Leal, M. T. (2006). A practical demonstration of water disinfection using TiO2 films and sunlight. *Water Research*, *40*(17), 3274–32802006. doi:10.1016/j.watres.2006.07.006 PMID:16949121

Gong, D., Grimes, C. A., Varghese, O. K., Hu, W., Singh, R. S., Chen, Z., & Dickey, E. C. (2001). Titanium oxide nanotube arrays prepared by anodic oxidation. *Journal of Materials Research*, *16*(12), 3331–3334. doi:10.1557/JMR.2001.0457

He, D. Q., Zhang, Y. J., Pei, D. N., Huang, G. X., Liu, C., Li, J., & Yu, H. Q. (2020). Degradation of benzoic acid in an advanced oxidation process: The effects of reducing agents. *Journal of Hazardous Materials*, *382*, 121090. doi:10.1016/j.jhazmat.2019.121090 PMID:31476718

Huang, S., Ning, C., Peng, W., & Dong, H. (2012). Anodic formation of Ti nanorods with periodic length. *Electrochemistry Communications*, *17*, 14–17. doi:10.1016/j.elecom.2012.01.011

Johns, P., Roberts, M., & Owen, J. (2011). Conformal electrodeposition of manganese dioxide onto reticulated vitreous carbon for 3D microbattery applications. *Journal of Materials Chemistry*, *21*(27), 10153. doi:10.1039/c0jm04357e

Khvan, S. V., Kim, J., Hong, S. C., & Lee, S. S. (2011). Large scale vertical implantation of crystalline titania nanotube arrays. *Journal of Industrial and Engineering Chemistry*, *17*(5-6), 813–817. doi:10.1016/j.jiec.2011.08.002

Kwon, Y., Kim, H., Lee, S., Chin, I. J., Seong, T. Y., Lee, W. I., & Lee, C. (2012). Enhanced ethanol sensing properties of TiO2 nanotube sensors. *Sensors and Actuators. B, Chemical*, *173*, 441–446. doi:10.1016/j.snb.2012.07.062

Lai, Y., Gong, J., & Lin, C. (2012). Self-organized TiO2 nanotube arrays with uniform platinum nanoparticles for highly efficient water splitting. *International Journal of Hydrogen Energy*, *37*(8), 6438–6446. doi:10.1016/j.ijhydene.2012.01.078

Lei, B., Luo, Q., Sun, Z., Kuang, D., & Su, C. (2013). Fabrication of partially crystalline TiO_2 nanotube arrays using 1, 2-propanediol electrolytes and application in dye-sensitized solar cells. *Advanced Powder Technology*, *24*(1), 175–182. doi:10.1016/j.apt.2012.05.005

Li, H., Qu, J., Cui, Q., Xu, H., Luo, H., Chi, M., Meisner, R. A., Wang, W., & Dai, S. (2011). TiO2 nanotube arrays grown in ionic liquids: High-efficiency in photocatalysis and pore-widening. *Journal of Materials Chemistry*, *21*(26), 9487–9490. doi:10.1039/c1jm11540e

Li, Y., Li, L., Li, C., Chen, W., & Zeng, M. (2012). Carbon nanotube/titania composites prepared by a micro-emulsion method exhibiting improved photocatalytic activity. *Applied Catalysis A, General*, *427-428*, 1–7. doi:10.1016/j.apcata.2012.03.004

Liang, F., Luo, L. B., Tsang, C. K., Zheng, L., Cheng, H., & Li, Y. Y. (2012). TiO_2 nanotube-based field effect transistors and their application as humidity sensors. *Materials Research Bulletin*, *47*(1), 54–58. doi:10.1016/j.materresbull.2011.10.006

Liu, N., Lee, K., & Schmuki, P. (2012). Small diameter TiO_2 nanotubes vs. nanopores in dye sensitized solar cells. *Electrochemistry Communications*, *15*(1), 1–4. doi:10.1016/j.elecom.2011.11.003

Liu, Y., Wang, H., Li, H., Zhao, W., Liang, C., Huang, H., & Shen, H. (2011). Length-controlled synthesis of oriented single-crystal rutile TiO2 nanowire arrays. *Journal of Colloid and Interface Science*, *363*(2), 504–510. doi:10.1016/j.jcis.2011.08.003 PMID:21872878

Meng, X., Banis, M. N., Geng, D., Li, X., Zhang, Y., Li, R., Abou-Rachid, H., & Sun, X. (2013). Controllable atomic layer deposition of one-dimensional nanotubular TiO_2. *Applied Surface Science*, *266*, 132–140. doi:10.1016/j.apsusc.2012.11.116

Momeni, M. M., Taghinejad, M., Ghayeb, Y., Bagheri, R., & Song, Z. (2019). Preparation of various boron-doped TiO_2 nanostructures by in situ anodizing method and investigation of their photoelectrochemical and photocathodic protection properties. *Journal of the Indian Chemical Society*, *16*(9), 1839–1851. doi:10.1007/s13738-019-01658-7

Nakata, K., & Fujishima, A. (2012). TiO2 photocatalysis: Design and applications. *Journal of Photochemistry and Photobiology C, Photochemistry Reviews*, *13*(3), 169–189. doi:10.1016/j.jphotochemrev.2012.06.001

Nguyen, C. H., Tran, M. L., Van Tran, T. T., & Juang, R. S. (2020). Enhanced removal of various dyes from aqueous solutions by UV and simulated solar photocatalysis over TiO_2/ZnO/rGO composites. *Separation and Purification Technology*, *232*, 115962. doi:10.1016/j.seppur.2019.115962

Nie, J., Mo, Y., Zheng, B., Yuan, H., & Xiao, D. (2013). Electrochemical fabrication of lanthanum-doped TiO_2 nanotube array electrode and investigation of its photoelectrochemical capability. *Electrochimica Acta*, *90*, 589–596. doi:10.1016/j.electacta.2012.12.049

Ortega-Díaz, D., Fernández, D., Sepúlveda, S., Lindeke, R. R., Pérez-Bueno, J. J., Peláez-Abellán, E., & Manriquez, J. (2020). Preparation of nanoparticulate TiO_2 containing nanocrystalline phases of anatase and brookite by electrochemical dissolution of remelted titanium components. *Arabian Journal of Chemistry*, *13*(1), 2858–2864. doi:10.1016/j.arabjc.2018.07.015

Palmas, S., Da Pozzo, A., Delogu, F., Mascia, M., Vacca, A., & Guisbiers, G. (2012). Characterization of TiO2 nanotubes obtained by electrochemical anodization in organic electrolytes. *Journal of Power Sources*, *204*, 265–272. doi:10.1016/j.jpowsour.2012.01.007

Roy, P., Berger, S., & Schmuki, P. (2011). TiO2 nanotubes: Synthesis and applications. *Angewandte Chemie*, *50*(13), 2904–2939. doi:10.1002/anie.201001374 PMID:21394857

Shankar, K., Mor, G. K., Paulose, M., Varghese, O. K., & Grimes, C. A. (2008). Effect of device geometry on the performance of TiO2 nanotube array-organic semiconductor double heterojunction solar cells. *Journal of Non-Crystalline Solids, 354*(19-25), 2767–2771.

Souza Filho, A. G., & Fagan, S. B. (2011). Nanomaterials properties. In *Nanostructured Materials for Engineering Applications* (pp. 5–21). Springer Berlin Heidelberg. doi:10.1007/978-3-642-19131-2_2

Tian, Z. R., Voigt, J. A., Liu, J., McKenzie, B., & Xu, H. (2003). Large oriented arrays and continuous films of TiO2-based nanotubes. *Journal of the American Chemical Society*, *125*(41), 12384–12385. doi:10.1021/ja0369461 PMID:14531662

Wang, J., & Zhuan, R. (2020). Degradation of antibiotics by advanced oxidation processes: An overview. *The Science of the Total Environment*, *701*, 135023. doi:10.1016/j.scitotenv.2019.135023 PMID:31715480

Wang, Q., Yang, X., Wang, X., Huang, M., & Hou, J. (2012). Synthesis of N-doped TiO_2 mesosponge by solvothermal transformation of anodic TiO2 nanotubes and enhanced photoelectrochemical performance. *Electrochimica Acta*, *62*, 158–162. doi:10.1016/j.electacta.2011.12.009

Wang, Y., Bi, N., Zhang, H., Tian, W., Zhang, T., Wu, P., & Jiang, W. (2020). Visible-light-driven photocatalysis-assisted adsorption of azo dyes using Ag_2O. *Colloids and Surfaces. A, Physicochemical and Engineering Aspects*, *585*, 124105. doi:10.1016/j.colsurfa.2019.124105

Yoon, J. H., Jang, S. R., Vittal, R., Lee, J., & Kim, K. J. (2006). TiO2 nanorods as additive to TiO2 film for improvement in the performance of dye-sensitized solar cells. *Journal of Photochemistry and Photobiology A Chemistry*, *180*(1-2), 184–188. doi:10.1016/j.jphotochem.2005.10.013

Yu, Y., Zhao, Y., Li, K., Zhang, G., Yu, K., Ma, Y., & Li, Y. (2020). Microstructures and optical properties of TiO_2/ZrO_2 nanotube/nanoporous heterofilm prepared by anodizing of Ti/Zr/Ti multilayer films. *Applied Surface Science*, *503*, 144316. doi:10.1016/j.apsusc.2019.144316

Zamudio Torres, I., Perez Bueno, J. J., Torres López, C. Y., Lartundo Rojas, L., Mendoza López, M. L., & Meas Vong, Y. (2016a). Nanotubes with anatase nanoparticulate walls obtained from NH_4TiOF_3 nanotubes prepared by anodizing Ti. *RSC Advances*, *6*(47), 41637–41643. doi:10.1039/C6RA05738A

Zamudio Torres, I., Perez Bueno, J. J., Torres López, C. Y., Lartundo Rojas, L., Mendoza López, M. L., & Meas Vong, Y. (2016b). A phenomenon of degradation of methyl orange observed during the reaction of NH_4TiOF_3 nanotubes with the aqueous medium to produce TiO_2 anatase nanoparticles. *RSC Advances*, *6*(80), 76167–76173. doi:10.1039/C6RA15149C

Zhao, C., Wang, Z., Chen, X., Chu, H., Fu, H., & Wang, C.-C. (2020). Robust photocatalytic benzene degradation using mesoporous disk-like N-TiO_2 derived from MIL-125(Ti). *Chinese Journal of Catalysis*, *41*(8), 1186–1197. doi:10.1016/S1872-2067(19)63516-3

Zhiyong, Y., Ruiying, Q., Runbo, Y., Zhiyin, W., & Huanrong, L. (2020). Photodegradation comparison for methyl orange by TiO2, H2O2 and KIO4 *Environmental Technology (United Kingdom)*, *41*(5), 547–555. doi:10.1080/09593330.2018.1505962 PMID:30059265

Zhou, J., Zhou, Z., Gao, Y., Li, T., Zhang, M., Fu, X., & Liu, F. (2020). Treatment of folic acid wastewater by 3D Fe-N-TiO_2/AC photoelectrocatalysis system. *Water Science and Technology*, *80*(10), 1919–1930. doi:10.2166/wst.2020.012 PMID:32144224

José de Jesús Pérez Bueno was born in 1973 in Zacatecas, México. He has been developing both basic and applied research, at the CIDETEQ (Centro de Investigación y Desarrollo Tecnológico en Electroquímica, S.C.), in the following areas: Dr. Perez has been an advisor in several concluded theses: 70 Bachelor, 12 Master Degree, 6 PhDs, and hosted 5 Postdoctoral. His published papers are currently 64, which up to date have 600 citations. In addition, he had published 5 papers in national journals, 21 book chapters, and 4 books. His work includes a national patent granted in 2010 and 12 pending patent applications. He received 13 awards, such as three Alejandrina Awards granted by the Autonomous University of Querétaro – Mexico; 2010 TECNOS Award; and the prize of the Institute of Materials Research of the UNAM, both to his doctoral thesis in 2003 as well as co-advisor in 2010.

Ildefonso Zamudio Torres's experience includes the synthesis of semiconductor and ferroelectric materials, using electrochemical, chemical, and physical methods. These can be obtained as thin films, coatings, or powders. He has had the opportunity to collaborate with different researchers and working groups, and due to his commitment and dedication, he has been recognized as the principal author and co-author of different articles and book chapters, including a patent application. Actually, Dr. Zamudio works in the Universidad Juárez Autónoma de Tabasco, and has been nominated as Researcher Candidate in the National System of Researchers (NSR), as well as in the State System of Researchers (SSR), granted by the Council of Science and Technology of the State of Tabasco, CCyTET.

Maria Luisa Mendoza López was born in 1975 in Tlahuac, Mexico City, Mexico. Currently Professor at Instituto Tecnológico de Querétaro (Technologic Institute of Queretaro) in both Mechanical Engineering and Materials Engineering. She obtained in 2005 her Ph.D. in materials science at CINVESTAV-IPN Unidad Queretaro. Her research topics are focused in: composite materials, water treatment and recycling of materials. She particularly study approaches to the selection of materials by properties and design. Other topic studied are: colloidal silica electrophoretic deposition; Sol-gel coatings and organic polymer matrices for organic-inorganic hybrid compounds; Treatment of water contaminated with heavy metal ions by electrodeless deposition; Reverse opal structures to maximize and control the surface area of bulk materials focused on treating contaminated air and water; characterization of metal alloys; recycling of materials such as polymers and fly ash; and others.